Rotational excitation in scattering of hyperthermal NO from Pt(111).

Wiskerke, A.E.; Taatjes, C.A.; Kleyn, A.W.; Lahaye, R.J.W.E.; Stolte, S.; Bronnikov, D.K.; Hayden, B.E.

published in
Journal of Chemical Physics
1995

DOI (link to publisher)
10.1063/1.468565

document version
Publisher's PDF, also known as Version of record

"Dynamical" versus "statistical" rotational distributions in hyperthermal NO–Pt(111) scattering

C. A. Taatjes,[a] A. E. Wiskerke, and A. W. Kleyn
FOM-Institute for Atomic and Molecular Physics, Kruislaan 407, 1098 SJ Amsterdam, The Netherlands

(Received 5 May 1994; accepted 18 November 1994)

Rotational distributions from NO–Pt(111) scattering have been reported [Wiskerke *et al.*, J. Chem. Phys. **102**, 3835 (1995)]. At lower incoming energies (<1 eV) clear rotational rainbows are seen, but the distributions for higher energies approach Boltzmann distributions with apparent temperatures far exceeding the surface temperature. We compare here the NO–Pt(111) scattering distributions to the predictions of a simple statistical model. The model assumes randomization of the available energy, subject to (partial) conservation of parallel linear momentum and angular momentum about the surface normal. Some characteristics of the rotational and angular distributions which arise from such a statistical energy repartitioning are discussed and compared to experimental results. It is seen that a combination of peaked angular distributions and Boltzmann-type rotational distributions independent of the scattering angle are reproduced by a simple statistical calculation with partial conservation of parallel linear momentum. For the NO–Pt(111) system, it is shown that a complete description of the high-energy scattering requires specifically dynamical assumptions. The transition from ''dynamics'' to ''statistics'' most likely arises from a combination of increased averaging, resulting from a competition between scattering via different regions of the potential energy surface, and a weakening of the rainbow features, perhaps due to the onset of chattering collisions. © *1995 American Institute of Physics.*

I. INTRODUCTION

The study of molecule–surface collisions by molecular beam scattering methods has progressed to the point where extremely detailed measurements of (correlated) final rotational, vibrational and translational energy distributions from well-characterized collision events can now be obtained. At the same time, advances in computational techniques now allow intricate calculations of molecule–surface scattering with ever less stringent approximations, and potential energy interactions are calculated from first principles. Understanding the details of molecule–surface interactions has been fueled by the experimental observations of specific dynamical features in molecule–surface scattering, such as rotational rainbows[1–10] and angular momentum orientation.[8–15] Nonetheless, for some scattering systems even high-resolution measurements give rotational distributions which are statistical, characterizable by a single apparent temperature.[14–16] Unlike trapping-desorption measurements, the rotational temperatures of these distributions far exceed the surface temperature, and are in fact dynamical phenomena.

The lack of dramatic features in the energy distributions for these systems suggests that statistical partitioning may dominate the scattering process. In particular, one can postulate a long-lived intermediate state which allows energy to be redistributed among many degrees of freedom, but which ''decomposes'' (i.e., the molecule departs from the surface) before complete thermal accommodation occurs. Statistical theories have previously been applied to state distributions from NO–graphite and NO–Ag(111) scattering by Pettersson *et al.*;[17–19] we here use a similar statistical assumption to describe scattering from a metal surface with a deep well, namely NO–Pt(111).[16,20–22] The deep attractive interaction offers the possibility that the molecule experiences several collisions with the surface, randomizing its energy among a few nearby surface atoms. This sort of indirect scattering may approximate the creation of a local ''complex.'' In the NO–Pt(111) experiments, a majority of the incoming molecules stick to the surface. These molecules fully equilibrate with the surface and later desorb. The scattering distributions that we describe here arise from a minority channel, those molecules which retain enough translational energy to escape after at most a few encounters with the surface.

While dramatic rotational rainbow features appear in low-energy (0.3–1 eV) NO–Pt(111) scattering, the rotational distributions at higher incident energies (1.6 eV) approach Boltzmann distributions, indicating a thorough redistribution of the available energy. The distributions are not thermal; the apparent temperatures are far above the surface temperature of 575 K. However, the randomization of the energy suggests a statistical description of the scattering process. Other treatments based on a statistical model for energy distribution have been previously applied to atom-and molecule–surface scattering processes.[17–19,23–25] In this article we will discuss how statistical the NO–Pt(111) distributions in fact are; in particular, whether these distributions can be adequately described by a random redistribution of energy subject to a few simple constraints. We will see that, while the qualitative features of the measured angular and rotational distributions are mimicked by a simple statistical model, a more nearly quantitative description requires other, dynamical couplings.

[a]Present address: Combustion Research Facility, Sandia National Laboratories, Livermore, California 94551-0969.

 0021-9606/95/102(9)/3848/12/$6.00

II. STATISTICAL DESCRIPTIONS OF SCATTERED DISTRIBUTIONS

The central idea of a statistical description of the scattering process is that, whatever the detailed form of the molecule–surface interaction, the scattering process can be represented as the decay of an local complex, where all the available states of a subsystem are populated with equal probability.[26–29] The calculation of the state distribution is thus reduced to calculating densities of states; ''counting'' the available states at a given total energy. The problem arises from deciding what parts of the total molecule–surface system are to be included in this ''activated complex,'' that is, what constraints are to be placed on the transport of energy. With no constraints the final state distribution would be given simply by the equilibrium distribution at the surface temperature. We are interested in cases where the equilibration is not so thorough, so we look at some ways to restrict the subsystem over which we will parcel the energy. In this section we shall outline some options for constraining the energy redistribution. A sketch of some mathematical derivations is given in the Appendix.

Nyman *et al.*,[18] Zamir and Levine,[23] and, most recently, Pettersson[19] have treated statistical distributions in molecule–surface scattering and have given expressions for the rotational state distributions. They use, as we do, a simple description of the surface (or at least the part of the surface that is involved in the scattering) as a collection of n classical harmonic oscillators, whose density of states as a function of energy, $\rho_{\rm osc}(E_{\rm osc})$ is proportional to $(E_{\rm osc})^{n-1}$. (The relevant part of the densities of states for calculation of final state distributions is their dependence on the energy; therefore for simplicity we will suppress constant factors in this discussion.) The density of states for a classical linear rotor is constant with rotational energy $E_{\rm rot}$. The translational density of states depends on how many dimensions are allowed for the translation (e.g., parallel momentum conservation implies a one-dimensional translational contribution), as well as whether flux or volume densities are calculated (these differ of course by a factor of velocity $\propto E_{\rm trans}^{1/2}$). The rotational energy distribution is then given by the integral over all the available states at a given energy,

$$P(E_{\rm rot})=\frac{\rho_{\rm rot}(E_{\rm rot})\int_0^{E-E_{\rm rot}} d\epsilon\,\rho_{\rm osc}(\epsilon)\rho_{\rm trans}(E-E_{\rm rot}-\epsilon)}{\int_0^{E} dE_{\rm rot}\rho_{\rm rot}(E_{\rm rot})\int_0^{E-E_{\rm rot}} d\epsilon\,\rho_{\rm osc}(\epsilon)\rho_{\rm trans}(E-E_{\rm rot}-\epsilon)}. \tag{1}$$

The energy distribution for any of the other degrees of freedom (translation, surface oscillators) is calculated in an identical manner, with the density of states for the desired degree of freedom [$\rho_{\rm trans}(E_{\rm trans})$, $\rho_{\rm osc}(E_{\rm osc})$] appearing outside the integral in the numerator. Since the rotational and translational densities of states have the same energy dependence, the rotational and translational temperatures will be identical in a completely statistical process. In other words, rotation and translation are *completely equivalent* in a statistical redistribution, unless other constraints (such as parallel angular momentum conservation) are introduced.

To give a J-distribution we ''bin'' the rotational energies by integrating the rotational energy distribution from $E_{\rm rot}=J^2b$ to $E_{\rm rot}=(J+1)^2b$ [i.e., truncating $J=(E_{\rm rot}/b)^{1/2}$ to an integer], where $b=h^2/2I$ is the rotational constant of the molecule with moment of inertia I. For the simple case of complete parallel momentum conservation, the (one-dimensional) translational density of states is proportional to $E_{\rm trans}^{-1/2}$, and the rotational energy distribution can be analytically calculated.[18,19] The rotational state distribution (for density detection) is then given by

$$P(J)=\int_{E_J}^{E_{J+1}} dE_{\rm rot}P(E_{\rm rot})$$
$$=\left(1-\frac{E_J}{E}\right)^{n+1/2}-\left(1-\frac{E_{J+1}}{E}\right)^{n+1/2}, \tag{2}$$

where the total available energy E is given by the perpendicular energy, $E_\perp=E_i\cos^2\Theta_i=E_i/2$ for the incident angle of 45° used in the NO–Pt(111) experiments,[16] plus any initial thermal excitation of the rotor and the surface oscillators. If the increase in available energy due to initial thermal excitation of n classical oscillators is included, we arrive at $E=E_\perp+nkT_s$. Since the oscillators are in some sense fictitious constructs, their initial excitation is somewhat arbitrary. This fact has been exploited by Nyman *et al.*, who chose the initial excitation using the oscillator frequency and a ''surface mass'' parameter,[18] and by Zamir and Levine, who ignored the initial oscillator excitation altogether.[23] For flux detection, the translational density of states is multiplied by the velocity, and the exponent in Eq. (2) becomes $n+1$ instead of $n+1/2$. The flux rotational distribution is a decreasing function of J for all values of n, but because of the inverse-velocity weighting, $P(J)$ for density detection actually increases with J for $n<1/2$.

A. Conservation of normal angular momentum

Nyman *et al.* have pointed out that requiring conservation of J_z (the angular momentum component along the surface normal) in the scattering process gives rise to a curvature in a Boltzmann plot of the rotational distribution near the high-energy cutoff.[18] Pettersson has recently carried out a detailed analysis of the effects of angular momentum conservation on statistical rotational distributions, and compared the results to experiments on NO–Ag(111) scattering.[19] J_z conservation produces a bulge in the Boltzmann plot, which is reminiscent of a rotational rainbow feature but has a much simpler origin. A constraint on J_z is related to the constraint of parallel momentum conservation, since both assume that the surface is in some sense ''smooth.'' Requiring that J_z is conserved necessitates an alteration in the procedure for calculating the rotational distribution. Nyman *et al.* used a Monte Carlo sampling technique. However, the problem can also be solved by calculating the conditional distribution for a given value of $J_z\equiv M_{\rm initial}$ and subsequently integrating (summing) over the initial M distribution. (The calculation of the final rotational distribution is treated in more detail in the Appendix.) The rotational density of states $\rho_{\rm rot}$ must be reduced by a factor which reflects the contribution of a single M value, relative to the isotropic density of states. Quantum mechanically, this is a factor of $(2J+1)^{-1}$. For continuous J we choose a density of states which will accomplish a

$(2J+1)^{-1}$ reduction in the available state density for a given J [i.e., for energies between J^2b and $(J+1)^2b$]. The density of states must therefore be multiplied by $(2J)^{-1} \propto (E_{\rm rot})^{-1/2}$, which is equivalent to using a one-dimensional rotor in the calculations of the state density.[19] This negative energy dependence of the effective density of rotational states produces a colder final rotational distribution, since the higher J states occupy a smaller region in the available phase space than when J_z is not conserved. The final rotational distribution is expressed in terms of Euler integrals [Eq. (A9)], which we calculate numerically.[30] In addition, partial conservation of J_z can be described by a less-drastic reduction in the density of rotational states with energy. As discussed in the Appendix, we can in general use a rotational density of states which is proportional to $E_{\rm rot}^{-\xi}$, where $\xi=1/2$ corresponds to complete J_z conservation, and $\xi=0$ to complete randomization of J_z.

A qualitative understanding of the source of the J_z-conservation "rainbow"[18,19] will help to illuminate the differences between this phenomenon and the true, dynamical rainbow feature. Figure 1(a) shows a rotational distribution calculated using the J_z-conserving assumption, with three features noted; a swift falloff with J at low rotational levels, a flattening at intermediate J, and a cutoff at the highest J. Between the flat part of the distribution and the high-J cutoff is the J_z-conservation pseudorainbow. The falloff at low J is due to the finite $T_{i,\rm rot}$ of the beam. The distribution in the figure was calculated for $kT_{i,\rm rot} \ll E$ in order to separate the three features clearly. For $kT_{i,\rm rot}$ closer to the total available energy, the features merge and blur, and under these conditions the distribution more resembles a weak rotational rainbow. In addition, as the number of surface oscillators is increased, the distribution approaches a Boltzmann distribution, as discussed by Pettersson.[19] The linear plot in Fig. 1(b) shows that the pseudorainbow does not produce the double-peaked "bimodal" distributions that are characteristic of many observed rainbow distributions. The distribution without J_z conservation is also shown for comparison.

The population in a particular J-state, J_f, in the statistical calculation, including J_z conservation, is partially determined by the initial M-population. If the initial rotational temperature approaches zero, then only the $M_f=0$ states can be populated. This is $1/(2J_f+1)$ of the possible M-population, so the high-J_f states are more greatly affected. Averaging over initial M causes the lower rotational levels, in the low-J falloff, to be most closely dependent on the initial rotational temperature.[19] At the highest J-levels, the energetic cutoff reduces the populations faster than exponentially. The bulge in the rotational distribution is caused when the flattening of the distribution, which occurs as $\langle J_i \rangle/(2J_f+1)$ depends less steeply on $E_{\rm rot}$, is overcome by the effect of the energetic cutoff. Therefore, the position of the pseudorainbow will always be near the energetic maximum. For a dynamical rainbow this is not necessarily true. One striking example is the CO–Ni(111) system, where the rainbow (attributed to O-end collisions) appears at moderate rotational energies, even though rotational excitation (presumably from C-end collisions) is observed up to the energetic limit.[7] In addition, since the statistical distributions de-

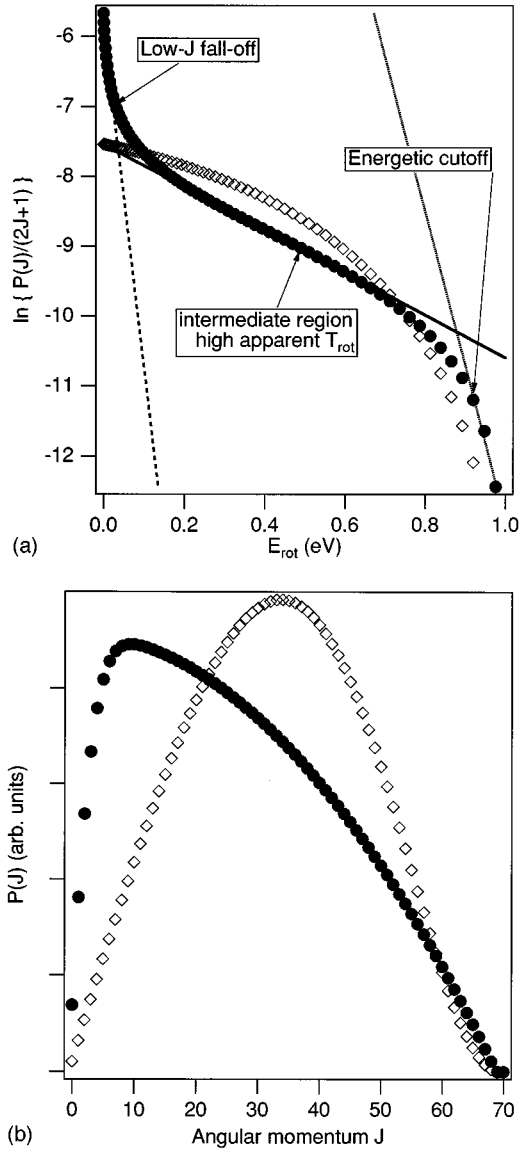

FIG. 1. (a) Statistical J_z-conserving ($\xi=0.5$, solid circles) rotational state distribution for initial rotational temperature $T_{i,\rm rot}$ = 75 K, $E=E_i=1.0$ eV, $n=1$, and $\beta=0.125$. Three distinct regions of the distribution are marked, and the straight lines are meant to guide the eye. The distribution obtained without J_z conservation is shown ($\xi=0$, open diamonds) for comparison. The two distributions have not been normalized and have been shifted for clarity. (b) The same distributions shown in a linear plot. The deviation of the J_z conserving case from a Boltzmann distribution is clear, but no obvious "bimodality" appears.

pend on *relative* energies, the energy of the pseudorainbow will be proportional to the total available energy. That is, a doubling of the available energy will result in a doubling of the energy at which the pseudorainbow occurs.

A direct measure of M-populations in molecule–surface scattering is given by the measurement of alignment moments of the scattered distribution. The moments are defined so that a positive value of the alignment moment $A_0^{\{2\}}$ corresponds to a preference for a "helicopter-type" motion (**J** parallel to the surface normal **n**), and a negative alignment to a preference for "cartwheel" motion ($\mathbf{J} \perp \mathbf{n}$).[11,31] The predicted alignment from a J_z-conserving approximation is easily explained. For low initial rotational temperatures, the

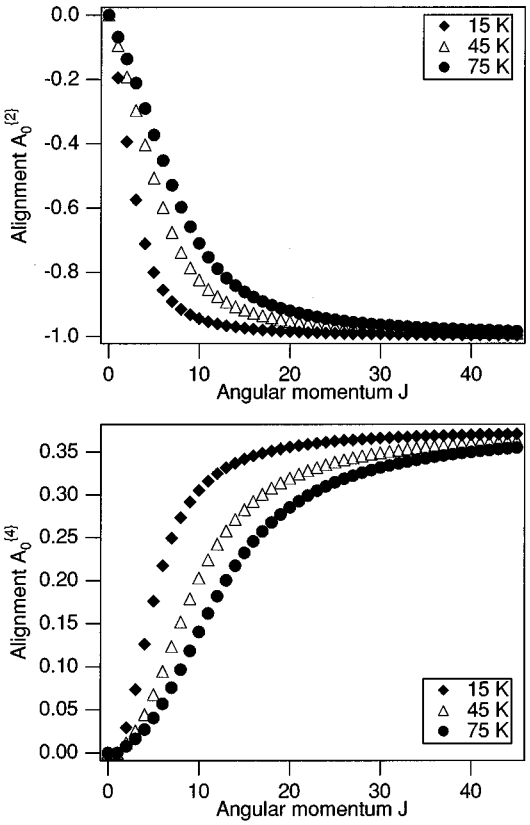

FIG. 2. Quadrupole alignment $A_0^{\{2\}}/A_0^{\{0\}}$ and hexadecapole alignment $A_0^{\{4\}}/A_0^{\{0\}}$ arising from a complete J_z-conserving statistical distribution, calculated for different initial rotational temperatures. Other parameters are the same as in Fig. 1. The definition of the alignment parameters is that of Kummel, Sitz, and Zare (Ref. 31).

alignment will start at zero for low J and decrease monotonically to its maximum negative value as J increases and the initial, allowed set of M-values becomes smaller relative to the $(2J+1)$ possible values. In all cases, cartwheel motion will be preferred. In Fig. 2 we show examples of the calculated alignment moments from several statistical distributions with J_z conservation. It should be noted that these alignment moments take no account of depolarization by fine or hyperfine structure, and comparison to real systems may have to take these effects into account.[31] The initial rotational temperature affects the swiftness of the approach to the maximum alignment in the intuitively expected manner—lower $T_{\rm rot}$ gives stronger alignment. Experimental measurements of the alignment in many systems show an increasingly negative quadrupole alignment, and an increase in the hexadecapole moment, with increasing J.[11–15] However, a positive alignment at low J has often been observed experimentally,[11–15] and the alignment moments do not go to their maximum values as quickly as those in Fig. 2. The calculation of alignment for partial J_z conservation requires a form for the final M-distribution [Eq. (A12)], but the qualitative result is obvious—weaker J_z conservation will slow the approach to a maximum alignment and will effectively decrease the maximum value. The strength of the alignment gives an indication of the strictness of J_z conservation in the scattering process, but any observation of positive alignment requires an alternative dynamical source.

B. Partial conservation of parallel momentum

A final question concerns the role of parallel momentum in determining the energy distribution. In general, any loss of parallel momentum, $p_\parallel$, by the molecule is counteracted by a momentum gain in the phonons. The two limiting cases for the availability of phonon momentum (i.e., conservation of parallel momentum or randomization of parallel momentum) are easily calculated. They correspond essentially to the use of $E_\perp$ (for $p_\parallel$ conservation) or E_i (for $p_\parallel$ randomization) as the available translational energy in Eq. (2), and a change from n to $n+1/2$ in the exponent for $p_\parallel$ randomization (because of the additional translational dimension). The difficulty arises for the intermediate cases. The simplest constraint one can apply for parallel momentum transfer $q=\Delta p_\parallel=(p_{\parallel,f}-p_{\parallel,i})$ to the surface is that of an average magnitude (equivalently, an average value $\langle q^2\rangle$). The distribution of maximum entropy is then given by[24]

$$P(q)=\exp\left(\frac{-q^2}{\langle q^2\rangle}\right). \tag{3}$$

The final parallel energy at a given exit angle Θ_f is completely determined by the value of q. The density of translational states is therefore altered (see Appendix),

$$\rho_{\rm trans}(E_{\rm trans})\propto e^{-2M_{\rm NO}(\sqrt{E_{\rm trans}}\sin\Theta_f-\sqrt{E_i}\sin\Theta_i)^2/\langle q^2\rangle}. \tag{4}$$

We normalize to the total energy, and absorb the mass of the NO molecule ($M_{\rm NO}$) and the factor of 2 in the exponential, to give a new effective parallel energy accommodation coefficient $\beta=\langle q^2\rangle/2EM_{\rm NO}$. Complete parallel energy conservation is obtained when $\beta=0$, and for $\beta\to\infty$ no constraint is placed on the parallel momentum transfer. For atom–surface scattering Meyer and Levine have given a physical basis for the width of the parallel momentum transfer probability.[24] For molecule–surface scattering the situation is somewhat more complicated, and we have simply used our β as a general accommodation coefficient. The parameter β is approximately the width of the parallel energy distribution, in units of the total energy. The rotational distribution is calculated by substitution of the new translational density of states (4) into Eq. (1) and numerical integration.[32]

In addition to the rotational distributions, we must consider the angular distribution of the scattered particles and the correlations between final angle and rotational and translational energy. The angular distribution is simply given by the integral over all final states at a particular angle (see Appendix). The rotational and translational energy distributions as a function of angle for the partial parallel momentum conservation are simple, since the final angle has already been used to constrain the parallel energy (and to remove one variable of integration). For the complete parallel momentum conservation expression, Eq. (2), the final angle is determined by the final perpendicular translational energy through $\tan^2\Theta_f=(E_{\parallel,f}/E_{\perp,f})=(E_i\sin^2\Theta_i/E_{\perp,f})$. The conditional distribution for $P(J)$ at a given $E_{\perp,f}$ is easily calculated (for flux detection $n\to n+1/2$),[18,19]

$$P(J|E_{\perp,f}) = \left[1 - \frac{E_J}{(E - E_{\perp,f})}\right]^{n-1/2} - \left[1 - \frac{E_{J+1}}{(E - E_{\perp,f})}\right]^{n-1/2}. \quad (5)$$

If the total initial energy is given only by the initial translational energy (i.e., initial rotational and surface temperature→0) then the scattered distribution will be limited to the superspecular region, since any energy transfer will move the scattering angle closer to the surface. Intensity in the subspecular region requires energy transfer from the surface or from rotations.

III. COMPARISON WITH EXPERIMENTAL DISTRIBUTIONS

The rotational distributions which arise from scattering of NO from Pt(111) are reasonably well-described by Boltzmann distributions at higher (1.6 eV) energies for all outgoing angles, although some deviations still occur for high-Θ_f scattering.[16] In addition, the scattering at subspecular angles (30° out) gives Boltzmann distributions for incoming energies from 0.3 to 1.6 eV. These rotational distributions are well-fit by simple statistical calculations such as Eq. (2), which is not surprising—Boltzmann distributions are after all statistical. In order to judge how much insight into the scattering process is given by the statistical treatment, we must also look at the other data which are available, namely the angular dependence of the rotational and translational energy, and the total angular distribution. In particular, distributions based on conservation of parallel momentum must be incomplete, because conservation of parallel momentum is known to be a poor approximation for NO–Pt(111).[22] Deviation from total parallel momentum conservation in NO–Pt(111) can immediately be seen in the energy transfer ($\langle E_{\rm trans}\rangle/E_i$) distribution;[16,20,22] the angular distribution is also sensitive to the degree of parallel momentum accommodation.

The angular distributions which have been measured for NO–Pt(111) scattering show broad (FWHM~40°) distributions which peak near the specular direction.[16,22] The angular distribution which would arise from a completely statistical reapportionment of energy (including both parallel and perpendicular momentum) would of course be a $\cos\Theta_f$ distribution. The departure from the ''thermal'' limiting distribution implies some constraint on parallel momentum accommodation. Another striking feature of the scattered distribution which helps to illustrate the role parallel momentum must play in the scattering process is that the effective rotational temperature is nearly independent of the final scattering angle, whereas under parallel momentum conservation, the rotational distributions must cool towards the normal to conserve energy. Similar behavior has been seen recently for N_2–W(110) scattering.[14,15] Taken together, these two observations require a *partial* accommodation of parallel momentum.

Figure 3(a) shows angular distributions calculated for a partial accommodation of parallel angular momentum, as described in the previous section. In these calculations the incoming kinetic energy of 1.0 eV was taken as the total energy, and the thermal (575 K) surface energy and the initial rotational energy were ignored. The energy transferred to the surface can be controlled with the oscillator number n. Increasing n for a constant E tends to move the angular distribution towards the surface, but the effect is small. Because of the increase in available energy due to the initial thermal excitation of the surface oscillators, $E = E_i + nkT_s$, the β parameter must be decreased as n increases to maintain a similar angular distribution, as shown in Fig. 3(b). The change in β must maintain the product $E\beta$ at a constant fraction of the initial parallel energy $E_i \cos^2\Theta_i$. Angular distributions are therefore approximately the same for identical values of $E\beta/E_i$. Figure 3(b) also shows a comparison to the experimental NO–Pt(111) angular distributions.[21,22] The experimental angular distributions can be qualitatively reproduced with a scaled parallel energy accommodation parameter ($E\beta/E_i$) of approximately 0.125, which indicates an average parallel energy transfer of about 1/8 of the initial translational energy. The statistical distribution is peaked slightly closer to the surface normal than the experimental distribution, suggesting that more perpendicular energy is transferred into internal degrees of freedom (surface and rotor). In Ar–

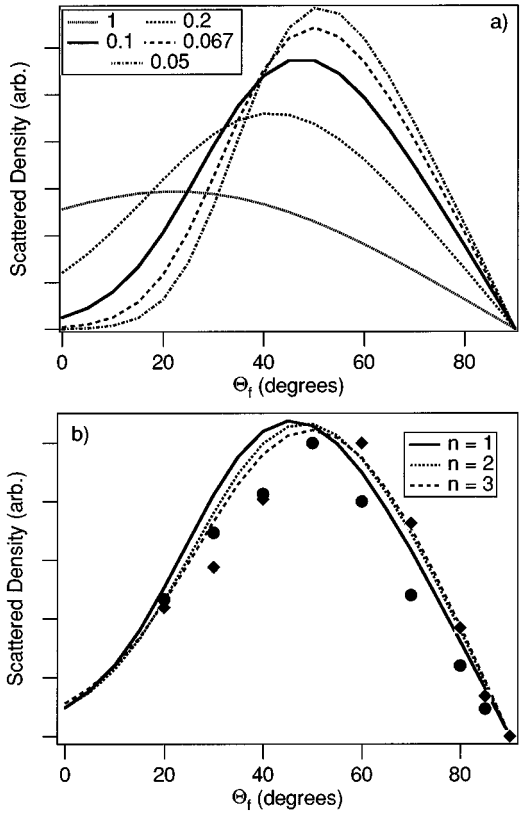

FIG. 3. (a) Angular distributions calculated using $E = E_i = 1$ eV, $n = 1$ for various values of the parallel accommodation parameter β. (b) Angular distributions for different numbers of surface oscillators n. Here we have used $E = E_i + nkT_s$ with $E_i = 0.3$ eV and $T_s = 575$ K, and scaled β, $E\beta/E_i \sim 0.125$. The solid line is $n = 1$, $\beta = 0.125$; dotted line, $n = 5$, $\beta = .074$; dashed line, $n = 10$, $\beta = 0.0625$. For comparison, experimental measurements of the angular distribution for NO–Pt(111) scattering are shown; circles represent $E_i = 1.5$ eV, diamonds $E_i = 0.4$ eV. In these distributions the incoming angle is 40°, and $\xi = 0$.

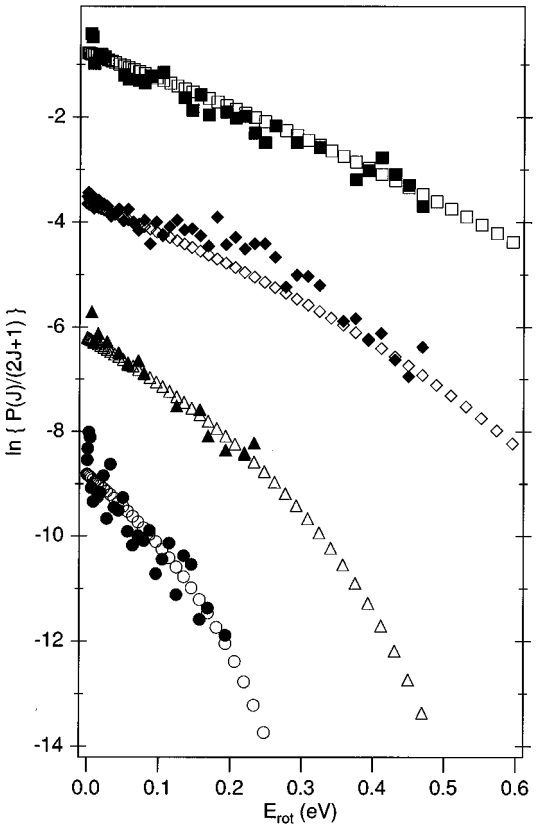

FIG. 4. Comparison of rotational state distributions from NO–Pt(111) scattering with statistical distributions calculated for partial parallel momentum conservation, $E\beta/E_i=0.125$. The normal angular momentum J_z is not conserved ($\xi=0$). The solid symbols are experimental data and the open symbols are the calculated distributions. Circles represent $E_i=0.34$ eV, $\Theta_f=30°$, triangles $E_i=0.53$ eV, $\Theta_f=30°$; diamonds $E_i=1.0$ eV, $\Theta_f=55°$, and squares $E_i=1.6$ eV, $\Theta_f=30°$. Unless otherwise mentioned, all distributions are for incoming angle $\Theta_i=45°$. The number of surface oscillators, n, for the statistical distributions is 0.34 eV $n=10$; 0.53 eV $n=7$; 1.0 eV $n=7$; 1.6 eV $n=8$. The distributions are vertically displaced from one another by three log units; the 0.53 eV distributions are not displaced.

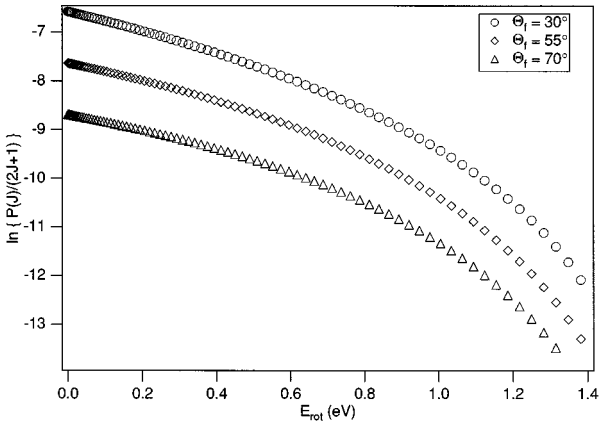

FIG. 5. Statistical rotational distributions calculated for $E\beta/E_i=0.125$, $E=E_i=1.6$ eV, $n=2$, $\xi=0$ for different exit angles Θ_f. The distributions differ by a few percent in average rotational energy for $\Theta_f=30°\langle E_{\rm rot}\rangle/E=0.205$; $\Theta_f=55°\langle E_{\rm rot}\rangle/E=0.208$; $\Theta_f=70°\langle E_{\rm rot}\rangle/E=0.215$.

Pt(111) scattering, it has been suggested that discrepancies between experiment and a simple ''modified cube'' model could be remedied by a constraint on the direction of parallel momentum transfer.[24] That would entail, in addition to our $\exp[-(\Delta p_\parallel)^2/\beta]$ factor, an additional constraint which depended on $\Delta p_\parallel$. It is possible that a similar refinement would improve the agreement in the present case.

The rotational distributions observed experimentally for NO–Pt(111) fall broadly speaking into two classes; Boltzmann-type distributions and rotational rainbow distributions. The Boltzmann-type distributions (low Θ_f and/or high E_i) are patently most amenable to a statistical explanation, so we shall concentrate on them. Figure 4 shows a comparison of some experimental rotational distributions from NO–Pt(111) scattering with simple statistical distributions calculated assuming partial parallel energy conservation, using a total energy $E=E_i+nkT_s$. The clearly ''dynamical'' rotational rainbow distributions have been left off this plot, but these features will be discussed below. The number of effective surface oscillators, n, required to adequately match the experimental distribution is larger than reported for the NO–Ag(111) system.[19] This suggests a difference in the scattering dynamics which is reflected in an increased coupling to the surface, perhaps that a larger portion of the surface is involved in the ''activated complex'' as the well depth increases.

At the highest incoming energies (1.6 eV), the apparent rotational temperature for NO scattered from Pt(111) is independent of the exit angle. This is similar to observations on N_2–W(110), where Boltzmann distributions have been reported which are independent of both incoming and outgoing angle.[14,15] The resemblance between the N_2–W(110) system at low to moderate incoming energies and the NO–Pt(111) at high energies is suggestive, since both systems have an attractive well, even though the N_2–W(110) chemisorption well is much shallower,[33] with a relatively small sticking probability. Yet the scattered angular distribution in these systems is not a cos Θ distribution, but is peaked around the specular direction.[22,34] In Fig. 5 statistical rotational distributions are given, using a β coefficient of $E\beta/E_i=0.125$, for the three exit angles (30°, 55°, and 70°) investigated experimentally. While some variation in average rotational energy is seen as a function of angle, this variation is well within the precision of the experimental measurements. It is apparent that the amount of parallel momentum accommodation which is necessary to wash out the angular variation in the average rotational energy is far smaller than that which is required to make the angular distributions approach the limiting cos Θ form. That is, explanation of a peaked angular distribution in conjunction with angle-independent rotational distributions requires no stronger dynamical constraint than a restriction on the average parallel energy transfer.

The final test of the quality of the statistical description of the experiment comes from the match with the translational energy observed at a given angle. The energy transfer, $\langle E_{\rm trans}\rangle/E_i$, in the NO–Pt(111) system is relatively flat with angle at approximately 50%.[21,22] This level of translational energy accommodation requires that a small number of ef-

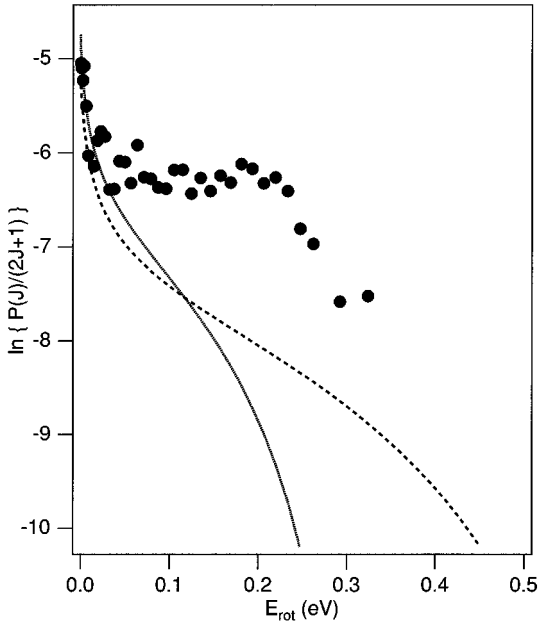

FIG. 6. Comparison of statistical J_z-conserving (ξ=0.5) rotational distributions for total energy $E=E_i$ of 0.6 eV (dashed line) and 0.3 eV (solid line), $n=2$, $E\beta/E_i=0.125$ with the experimental distribution for $E_i=0.53$ eV, $\Theta_f=70°$, which shows a clear rotational rainbow. This dynamical effect cannot be reproduced by simple statistical calculations.

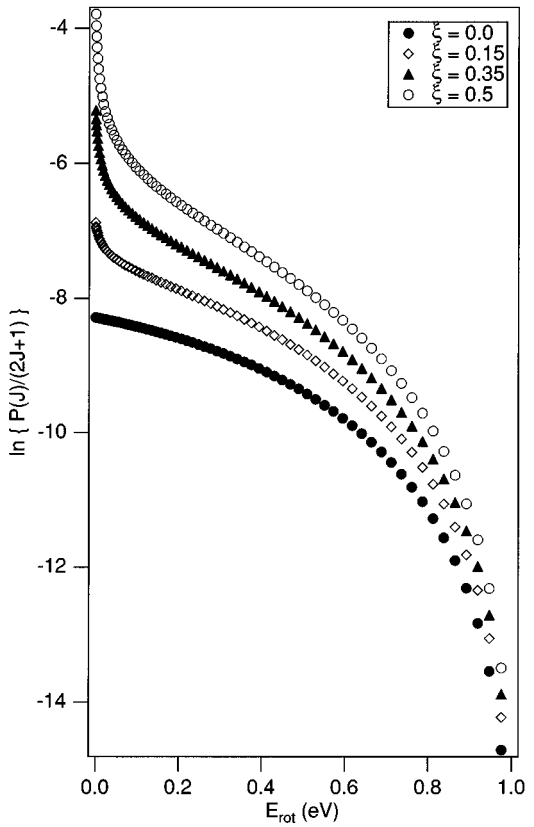

FIG. 7. Calculated rotational distributions for $E=E_i=1.0$ eV, $n=2$, $E\beta/E_i=0.125$ using various degrees of partial J_z conservation. The parameter ξ=0 for no J_z conservation, and ξ=0.5 for complete J_z conservation. See text for details.

fective surface oscillators are used in the statistical calculations. On the other hand, use of a small number of surface oscillators would predict a rotational distribution which is far too hot. If the angular distributions and the rotational distributions are fit using a particular value of n and of β, then the final translational energy which is predicted is far too small. Evidently the statistical calculations we have discussed cannot reproduce all the features of the observed distributions simultaneously, even at high E_i. Some other dynamical constraint is clearly operating in the scattering process, a constraint which acts to reduce the rotational excitation relative to the translation.

One such constraint has been previously mentioned, namely the conservation of the angular momentum about the surface normal, J_z. This has the effect of removing energy from the rotational degrees of freedom, as mentioned in the previous section. The rotational distribution also changes shape, as other investigators have noted;[18,19] it has been suggested that some of the rotational rainbow features which have attracted so much attention in the field of molecule–surface scattering could be explained by this statistical effect. In the previous section we discussed the shape of the distributions which arise from J_z-conservation. It is clear that the maxima and other high-J features observed at lower energies in the NO–Pt(111) system cannot be explained by simple J_z conservation. Figure 6 shows J_z-conserving distributions corresponding to $E=0.3$ and 0.6 eV ($E_\perp$ and E_i), compared with the experimental distribution for $\Theta_i=70°$, incident energy $E_i=0.53$ eV. The high-J features are not reproduced by J_z-conserving statistical distributions, and require explicit dynamical interpretation. The most straightforward interpretation is that the maxima arise from a dynamical constraint on rotational excitation in the NO–Pt collision. Such a constraint is also known as a rotational rainbow, or dynamically-constrained maximum in rotational excitation.

On the other hand, the reduction in the average rotational energy implied by J_z conservation suggests that perhaps the high-energy scattering can still be described by a low number of surface oscillators, but by invoking (partial) J_z conservation, the rotational temperatures can be lowered to be in accordance with experiment. Figure 7 shows some rotational distributions which have been calculated for varying degrees of J_z conservation (i.e., differing values of the parameter ξ). The shape of the distribution changes gradually from the double-curved form of total J_z conservation to the single curve of the simple statistical distribution as ξ is decreased from 0.5 to 0. However, a cursory comparison of these distributions with the experimental distribution shows that, while the average rotational energy may be fit by a partial J_z conserving approximation, the shape of the distribution requires that J_z conservation play a minor role. Nonetheless, there appears in most of the NO–Pt(111) distributions a small overpopulation at low J which may arise from partial J_z conservation.[16] The observation of negative alignment for NO scattered from Pt(111) would seem to support this conclusion.[11] The experimentally observed alignment is smaller than that shown in Fig. 2, as would be expected for weak J_z conservation. A quantitative prediction for alignment moments for partial J_z conservation has not been cal-

culated; this would require a solution of Eq. (A12). The relaxation of the strict J_z conservation must reduce the alignment and retard the approach of the alignment parameter to its asymptotic value. Since the actual dynamical significance of the ξ parameter in our expressions is somewhat unclear, a more explicit calculation seems unwarranted.

Detailed comparison of the experimental distribution with the results of statistical calculations shows that the rotational and translational energy distributions cannot be simultaneously fit using the simple constraints we have proposed. The experimental results clearly indicate that the rotational and translational degrees of freedom cannot be treated as equivalent. In particular, the transfer of parallel momentum which is necessitated by the angular distributions and the translational energy disposal does not imply that a corresponding amount of parallel translational energy is made available for rotations. A similar conclusion has been drawn by Hanisco and Kummel for N_2–W(110) scattering.[14,15] In order to fit the kinetic energy, angular, and rotational distributions we would have to use different β parameters for parallel energy conservation in our calculations of each; this is essentially equivalent to enforcing a dynamical separation between the translational and rotational energy transfer. The features of the experimental distributions could be recovered with a smaller β for the rotational distribution than for the translation, corresponding to a higher probability for parallel energy to go into perpendicular translation than into rotation or into surface vibrations. In other words, there appears to be a higher lateral corrugation, which affects the motion of the molecule center-of-mass, than angular corrugation, which couples the parallel momentum to the rotation of the molecule. Alternatively, a larger n could be used for the calculation of the rotational distributions than for the translation. It should be emphasized that these alternatives, involving separate calculation of different degrees of freedom, have no direct physical meaning. They merely illustrate what type of dynamic constraint exists in the real system that has not been taken into account in the statistical description.

IV. DISCUSSION

The scattering of NO from a Pt surface shows a richness of behavior, from striking rotational rainbows to broad Boltzmann distributions. The transition between the type of behavior which would be expected from a single, highly dynamically constrained encounter with the surface (rotational rainbows, large dependence of rotational distributions on exit angle, i.e., ''dynamical'' scattering) to behavior more like that of a long-lived complex interaction (Boltzmann rotational distributions independent of exit angle, i.e., ''statistical'' scattering) occurs as the total incoming energy is raised to above the order of the chemisorption well. This is surprising, since the scattering as a whole must be less and less well-described by long-lived collisions as the incoming energy increases. But because of the large sticking probability for NO–Pt(111) (0.9 at $E_i = 0.3$ eV),[35] the molecules probed in the experiments are only a small fraction of the total incoming flux. The minority channel probed in the experiments, the promptly scattered fraction, exhibits this counterintuitive energy dependence, making a transition to a ''statistical'' distribution only at higher energies. The observation of statistical state distributions even for angle-resolved scattering with well-defined initial states indicates that the energy scrambling is characteristic of the scattering process itself. However, a simple redistribution of energy cannot, as we have seen in the previous section, simultaneously describe the rotational, angular, and translational energy distributions.

The low-energy scattering exhibits strong rotational rainbows at $\Theta_f > 45°$, but the distributions at 30° are Boltzmann-type for all incoming energies. As with any Boltzmann-type distribution, the 30° results can be fit by a statistical calculation. It is tempting to directly assign the subspecular scattering to molecules which enter the part of the potential surface associated with statistical scattering, and to assume that the nature of the 30° scattering at low energy is the same as that for all angles at higher energy. But, since the statistical calculations are by nature relative-energy calculations, the distribution in relative energy will be the same for different incoming energies if the scattering is statistical. The values of $\langle E_{\rm rot}\rangle/E_i$ for NO–Pt(111) show a slight but significant decrease with increasing E_i;[16] the rotational temperature is not exactly proportional to the incoming energy. For N_2 from W(110) there is a similar energy dependence,[14] suggesting corresponding scattering dynamics. If the fraction of the ''total'' energy is used, where the total energy is $E = E_i + nkT_s$ from the best statistical fit, the ratio $\langle E_{\rm rot}\rangle/E$ is more nearly flat with E.

Nevertheless, the similarity of the total angular distributions for all incoming energies undermines the idea that the low-energy subspecular scattering and the high-energy scattering at all angles arise from a single statistical channel, with identical constraints on the energy redistribution. The processes which give rise to the observed Boltzmann-type distributions change with increasing energy. This suggests that describing the Boltzmann-type scattering channel as the decay of a quasibound NO–Pt_n ''complex'' is flawed. It can be seen that care must be taken not to infer mechanistic information about the scattering process from partial data. Although the individual final energy distributions for NO–Pt(111) may appear statistical, the *complete* behavior of the scattering process, or even of an presumed ''Boltzmann channel,'' does not match the simple statistical predictions. It is therefore unlikely that the scattering of NO from Pt(111) in the observed energy range can be broken down into two simple pathways, one ''statistical'' and one ''dynamical.'' A similar point should be made about the NO–Ag(111) system, where the results of oriented molecule scattering have shown manifestly nonstatistical behavior,[3] despite the similarity of more highly averaged measurements to J_z-conserved statistical calculations.[19]

Any success of a statistical description of a molecule–surface scattering process must in the end be explained in terms of some underlying dynamical basis. The ''statistical'' nature of the process simply indicates a loss of memory as to the particular of the initial state, so that the final state distribution depends only on total energy (or a few other simple conserved quantities, as we have discussed). This corresponds to a loss of information about the shape of the inter-

action potential for differing initial states. In general, any averaging over initial conditions or final states will tend to make the process appear more ''statistical.'' For a thorough apparent randomization of the energy, it is necessary to have a strong variation in the final state for differing initial conditions, for example, high lateral or angular corrugation.[36] There are some averages which remain experimentally unavoidable, for example, averaging over impact parameter or surface site, and, in most cases, averaging over initial molecular orientation. In the case of NO–Pt(111) scattering, some increase in averaging almost certainly occurs as the energy increases; the sticking coefficient drops,[35] and molecules from additional surface sites or molecular orientations are added to the scattered distribution. This additional averaging must play some role in the transition from ''dynamics'' to ''statistics'' in NO–Pt(111) scattering.

Possible dynamical sources of a statistical distribution include multiple collisions and ''chattering'' collisions.[37] Multiple collisions, where the center of mass of the molecule approaches the surface more than once, have been seen for NO–Pt(111) in the classical trajectory studies of Jacobs and Zare.[38] Multiple collisions are very efficient in energy randomization, but their probability must decrease with increasing energy. With increasing energy it is likely that many multiple-collision trajectories which would have become bound to the surface now escape after fewer bounces. Multiple-collision scattering from the deep-well region of the potential surface can be presumed to be ''statistical'' collisions. If all of the increase in scattered flux between 0.34 and 1.6 eV arises from such indirect collisions, the randomized distributions could well overwhelm any remaining rainbow scattering. This added distribution is not completely described by a statistical energy disposal, as we have seen, but retains a dynamical separation of translational and rotational excitation. Similar submersion of the direct, single-collision, ''dynamical'' distribution in a multicollision ''statistical'' distribution, arising from scattering through the well, probably occurs in other systems where the well depth is large but the sticking probability is still significantly less than unity (see Table II of the preceding paper).

The onset of chattering, where both ends of the molecule strike the surface in rapid succession, before reversal of the center-of-mass motion, considerably reduces rotational excitation.[39] In a perfect chattering collision all of the translational energy is transferred to rotation on the initial impact, then back into translation as the other end strikes the surface, leaving the molecule with no rotational excitation. For initial conditions slightly different from the perfect chattering condition, it can be expected that the rotational excitation will vary widely. If a larger anisotropy exists for the interaction with the N-end of the molecule than for the O-end, chattering could set in at relatively low incoming energies for N-end collisions, while for O-end collisions a rotational rainbow is still evident. In addition, as we have discussed in previous publications,[16,20,21] selective trapping of the N-end collisions, seen in oriented molecule scattering studies,[40] amplifies the O-end rainbow feature. As the energy increases, not only do the N-end collisions, and collisions at different surface sites, begin to overwhelm the direct rainbow scattering, but eventually chattering will also set in for O-end collisions. The relative rotational excitation will then decrease with increasing energy, and the distributions will simultaneously become more ''statistical.''

In the NO–Pt(111) system, we have seen from the measured angular distributions and the comparisons with statistical models that the low-energy subspecular Boltzmann distributions arise from a qualitatively different scattering process than the high-energy Boltzmann distributions. It is known for NO–Pt(111) collisions at 0.24 eV that the O-end collisions dominate the superspecular scattering, whereas both N and O-end collisions contribute to the subspecular intensity.[40] Near-Boltzmann distributions have been seen in oriented NO–Ag(111) scattering for the preferred N-end approach.[3] This phenomenon was described in terms of a low-energy N-end rainbow by Voges and Schinke.[41] The Boltzmann distributions observed for a 30° exit angle in NO–Pt(111) could possibly arise from analogous effects. However, we have proposed an interaction potential for NO–Pt(111) which differs considerably from the Voges and Schinke NO–Ag(111) potential,[16,21] with a deep well at the N-end, reflecting the binding geometry of NO on Pt. The subspecular Boltzmann distributions using such a form for the potential will most likely arise from some kind of double-collision.

V. CONCLUSIONS

A simple statistical model has been put forward to describe the randomization of energy which is apparent in NO–Pt(111) scattering at higher energies. This model allows partial conservation of parallel linear momentum and of angular momentum along the surface normal. The predictions of the statistical model have been useful in separating what are general features of the distributions, arising from simple restrictions on the available phase space, from features which have dynamical sources specific to the NO–Pt(111) system. It has been shown that the simultaneous observation of peaked angular distributions and Boltzmann-type rotational distributions which are independent of the scattering angle is straightforwardly explained by a statistical model. In addition, rotational distributions which depart markedly from Boltzmann populations can be produced under conditions where the angular momentum about the surface normal is partially conserved. Such distributions display a characteristic low-J ''fall-off'' and can, under some conditions, mimic a weak rotational rainbow. However, the observed NO–Pt(111) distributions cannot be consistently explained by a simple statistical process, and clear indications are seen that the translational and rotational degrees of freedom do not have equal access to the initial parallel energy. The transition at higher incoming energies from ''dynamical'' to ''statistical'' distributions in NO–Pt(111) scattering appears to be due to a combination of increased averaging over a larger range of molecular orientations and/or surface sites, and the elimination of the dynamical rainbow channel, perhaps by chattering collisions.

ACKNOWLEDGMENTS

This work is part of the research program of the Stichting voor Fundamenteel Onderzoek der Materie (FOM), with financial support from the Nederlandse Organisatie voor Wetenschappelijk Onderzoek (NWO).

APPENDIX: MATHEMATICAL EXPRESSION OF STATISTICAL DISTRIBUTIONS

We assume that the surface can be described by a collection of n classical harmonic oscillators, with a total density of states

$$\rho_{\rm osc}(E_{\rm osc})=\frac{(E_{\rm osc})^{n-1}}{(n-1)!\Pi_{k=1}^{n}h\nu_k}. \tag{A1}$$

Here ν_k is the frequency of the kth oscillator, and h is Planck's constant. The actual frequencies of the oscillators are largely immaterial. The final energy distribution is affected only by the $E_{\rm osc}$ dependence of the density of states, and, since the oscillators are classical, their initial and final excitations are not quantized. The classical density of states for a linear rotor with moment of inertia I is

$$\rho_{\rm rot}(E_{\rm rot})=\frac{8\pi^2 I}{h^2}=b^{-1}, \tag{A2}$$

where b is the rotational constant. The density of translational states which we use depends on the number of translational degrees of freedom available. For complete parallel momentum conservation, translation in only one dimension is involved in the energy redistribution and we use the density of states for a one-dimensional translation,

$$\rho_{\rm trans}(E_{\rm trans})=\frac{1}{h}\left(\frac{M_{\rm NO}}{2E_{\rm trans}}\right)^{1/2}. \tag{A3a}$$

If the flux of molecules is to be measured, we must multiply by the velocity

$$\rho_{\rm trans}(E_{\rm trans})=\frac{1}{h}. \tag{A3b}$$

If there is no constraint on parallel momentum transfer, but we still look only at in-plane scattering, then the two-dimensional translational contribution is needed,

$$\rho_{\rm trans}(E_{\rm trans})=\frac{M_{\rm NO}}{h^2} \tag{A3c}$$

for density detection, and

$$\rho_{\rm trans}(E_{\rm trans})=\frac{(2E_{\rm trans}M_{\rm NO})^{1/2}}{h^2} \tag{A3d}$$

for flux detection.

The rotational distributions for the simple case of conservation of parallel momentum have been reported by other workers;[18,19,23] we turn our attention to the distributions that arise from other constraints on the partitioning of energy. For conservation of J_z we first calculate the rotational distributions that arise from the scattering of molecules with a single initial $J_z \equiv M$, as described in the text. The available state density is reduced to the amount contributed by a single value of the projection M, which is inversely proportional to J.[21] Hence the state density is divided by $2J=2(E_{\rm rot}/b)^{1/2}$;

$$\rho_{\rm rot}(E_{\rm rot}|M)=\frac{1}{2b}\left(\frac{b}{E_{\rm rot}}\right)^{1/2}=\frac{1}{2}\,(bE_{\rm rot})^{-1/2}. \tag{A4}$$

The integration over the state density is somewhat more complicated, but can be accomplished in terms of the Euler integrals,[19,42] which can be readily evaluated numerically.[30] We substitute Eq. (A4) into Eq. (1) and first perform the integral over the translational and oscillator energies (for density detection n must be replaced by $n-1/2$),

$$\begin{aligned} &P(E_{\rm rot}|M)\propto\frac{E_{\rm rot}^{-1/2}(E-E_{\rm rot})^n}{\int_0^E dE_{\rm rot}\rho_{\rm rot}(E_{\rm rot})(E-E_{\rm rot})^n}, \quad E_{\rm rot}\geqslant M^2 b,\\ &P(E_{\rm rot}|M)=0, \quad E_{\rm rot}<M^2 b. \end{aligned} \tag{A5}$$

But, since $\rho_{\rm rot}(E_{\rm rot})$ must be 0 for $J<M$, the normalization integral in the denominator will begin not at zero, but at the rotational energy which corresponds to $J=M$. This integral is easily rewritten in terms of Euler integrals. The results for the rotational energy distribution for a given initial M is given by (again, for density detection n must be replaced by $n-1/2$),

$$\begin{aligned} &P(E_{\rm rot}|M)=\frac{E_{\rm rot}^{-1/2}(E-E_{\rm rot})^n}{E^{n+1/2}B\left(\frac{1}{2},n+1\right)\left[1-I\left(\frac{M^2 b}{E};\frac{1}{2},n+1\right)\right]};\\ &M^2 b\leqslant E_{\rm rot}, \quad M^2 b\leqslant E_{i,\rm rot}, \end{aligned} \tag{A6}$$

where $B(x,y)$ is the Euler beta function (Euler integral of the first kind), which can be expressed in terms of the gamma function (Euler integral of the second kind), $B(x,y)=\Gamma(x)\Gamma(y)/\Gamma(x+y)$. $I(x;y,z)$ is the incomplete beta function,[42]

$$I(x;y,z)=\frac{\Gamma(y+z)\int_0^x t^{y-1}(1-t)^{z-1}dt}{\Gamma(y)\Gamma(z)}. \tag{A7}$$

The conditions on M^2 in Eq. (A6) require that M be less than or equal to both $J_{\rm initial}$ and $J_{\rm final}$; the probability is zero otherwise. Notice that for $M=0$ our result reduces to the case given by Pettersson.[19] The rotational state populations for a single M are given by integration over $E_J\leqslant E_{\rm rot}\leqslant E_{J+1}$ to give final J states (a truncation of M to an integer is implicit in this integration), which yields incomplete beta functions in the numerator,

$$\begin{aligned} &\int_{E_J}^{E_{J+1}}dE_{\rm rot}E_{\rm rot}^{-1/2}(E-E_{\rm rot})^n\\ &\quad=E^{n+1/2}B\left(\frac{1}{2},n+1\right)\left[I\left(\frac{E_{J+1}}{E};\frac{1}{2},n+1\right)\right.\\ &\qquad\left.-I\left(\frac{E_J}{E};\frac{1}{2},n+1\right)\right]. \end{aligned} \tag{A8}$$

The final rotational state distribution for total J_z-conservation can be analytically calculated; it is expressed as a sum over an initial rotational distribution

$$P(J)=\frac{1}{q_{\rm rot}(T_{i,\rm rot})}\sum_{J_i}\exp\left(-\frac{E_{J_i}}{kT_{i,\rm rot}}\right)\times\sum_{M=-\mu}^{\mu}\int_{E_J}^{E_{J+1}}dE_{\rm rot}P(E_{\rm rot}|M)$$
$$=\frac{1}{q_{\rm rot}(T_{i,\rm rot})}\sum_{J_i}\exp\left(-\frac{E_{J_i}}{kT_{i,\rm rot}}\right)\times\sum_{M=-\mu}^{\mu}\frac{I\left(\frac{E_{J+1}}{E};\frac{1}{2},N+1\right)-I\left(\frac{E_J}{E};\frac{1}{2},N+1\right)}{\left[1-I\left(\frac{M^2b}{E};\frac{1}{2},N+1\right)\right]}. \tag{A9}$$

Here $q_{\rm rot}(T_{i,\rm rot})$ is the rotational partition function at the initial rotational temperature $T_{i,\rm rot}$, $\mu\equiv\min(J_i,J)$, and k is the Boltzmann constant. The shapes of the distributions acquired in this manner agree well with the results reported for the Monte Carlo sampling method, and our result is identical to Pettersson's expression in the $T_{i,\rm rot}\rightarrow 0$ limit.[19] In our comparisons to the NO–Pt(111) data we assume that the rotational energy makes a negligible contribution to the total energy. (The rotational temperature in the experiments corresponds to less than 1% of the total energy.) We can then separate the Boltzmann factor in the rotational average from the integration and use the $M=0$ distribution as a basis for the complete distribution [since $I(0;y,z)=0$, Eq. (A9) is simplified]. The distribution for $M\neq 0$ is given by the $J\geqslant M$ terms of this distribution, renormalized to $[\Sigma\, P(J|M=0),J\geqslant M]$. We multiply this basis distribution by the probability of each (integral) M value in the initial thermal rotational distribution. The sum of these products then gives the total rotational distribution.

An expression for *partial* conservation of J_z can be constructed by allowing M to change, that is, by allowing a single $M_{\rm initial}$ state to have access to a larger fraction than $(2J+1)^{-1}$ of the total state density. This must be reflected in the energy dependence of the rotational density of states; so we use as a general case $\rho_{\rm rot}$ proportional to $E_{\rm rot}^{-\xi}$, where $\xi=0$ and $\xi=1/2$ correspond to no J_z-conservation and total J_z-conservation, respectively. This partial conservation can be rationalized by exploiting the analogy to a one-dimensional rotor pointed out by Petersson.[19]

The total density of states for the linear rotor can be represented as the convolution of two 1D rotors,

$$\rho_{\rm rot}(E_{\rm rot})=\int_0^{E_{\rm rot}}d\epsilon\,\rho_{\rm rot}^{\rm 1D}(E_{\rm rot}-\epsilon)\rho_{\rm rot}^{\rm 1D}(\epsilon), \tag{A10}$$

and the partial conservation of J_z is then a restriction on the state density of one rotor (the "z-rotor"),

$$\rho_{\rm rot}(E_{\rm rot})\propto\int_0^{E_{\rm rot}}d\epsilon(E_{\rm rot}-\epsilon)^{-1/2}\epsilon^{-(\xi+1/2)}$$
$$=E_{\rm rot}^{-\xi}B\left(\frac{1}{2},\frac{1}{2}-\xi\right). \tag{A11}$$

The final distribution of M for a given M_i and J, $f(M|J,M_i)$, can be written as the solution of an integral equation,

$$\int_J^{J+1}dj\int_{-j}^{j}dM f(M|j,M_i)=\int_{E_J}^{E_{J+1}}dE_{\rm rot}\rho_{\rm rot}(E_{\rm rot})=(J+1)^{2-2\xi}-J^{2-2\xi}, \tag{A12}$$

by requiring that the integrated final M probability distribution reflect the available state density. For partial J_z conservation, one can as a first approximation simply replace 1/2 wherever it appears in Eq. (A9) with the factor ξ, $0\leqslant\xi\leqslant 0.5$, introduced above. This approximation ignores the fact that the restriction $J_{\rm final}\geqslant M_{\rm initial}$ must also be relaxed, which affects the J-states with significant initial populations. We have removed the restriction in an ad hoc manner in our calculations by simply weighing the $J_{\rm final}<M_{\rm initial}$ portions of the distribution by a factor $(1-2\xi)\exp[\xi(J_{\rm final}-M_{\rm initial})]$. A "truer" weight for $J<M_{\rm initial}$ could in principle be obtained in conjunction with a solution of Eq. (A12), but since the initial rotational temperatures in the experiments are low, the details of how to include the $J_{\rm final}<M_{\rm initial}$ channels make little difference.

For partial conservation of parallel momentum, we need the density of translational states subject to the restriction on the probability of final parallel momenta [Eq. (3)]. We restrict ourselves to in-plane scattering, and so use the two-dimensional expression for the number of translational states between $E_{\rm trans}$ and $E_{\rm trans}+dE_{\rm trans}$ at an angle between Θ and $\Theta+d\Theta$, multiplied by the parallel momentum probability $\exp(-[\Delta p_\parallel]^2/\langle q^2\rangle)$,

$$\rho_{\rm trans}(E_{\rm trans})dE_{\rm trans}\,\frac{d\Theta}{\pi}=\frac{e^{-(\Delta p_\parallel)^2/\langle q^2\rangle}}{h^2}\,dp; \tag{A13}$$

$$\rho_{\rm trans}(E_{\rm trans})=\frac{\pi}{h^2}\,e^{-2M_{\rm NO}(\sqrt{E_{\rm trans}}\sin\Theta_f-\sqrt{E_i}\sin\Theta_i)^2/\langle q^2\rangle}p\,\frac{dp}{dE_{\rm trans}}$$
$$=\frac{\pi M_{\rm NO}}{h^2}\,e^{-2M_{\rm NO}(\sqrt{E_{\rm trans}}\sin\Theta_f-\sqrt{E_i}\sin\Theta_i)^2/\langle q^2\rangle}.$$

We absorb the $2M_{\rm NO}$ factor and normalize to the total energy to define a new accommodation coefficient $\beta=\langle q^2\rangle/2EM_{\rm NO}$. The β coefficient is related to the availability of the parallel kinetic energy for the other degrees of freedom; for $\beta=0$ the parallel momentum (and energy) is strictly conserved, and for $\beta\rightarrow\infty$ the parallel momentum is completely available for repartitioning (a $\cos\Theta_f$ angular distribution will then result).

Similar considerations apply to the calculation of angular distributions and the energy transfer, $\langle E_{\rm trans}\rangle/E_i$, as a

function of angle. Note that the expression for the angular distribution contains the factor $\cos\Theta_f$, which ensures that a complete accommodation of parallel momentum results in a cosine distribution.[43] This factor arises from the volume element for the scattered flux per unit area on the surface at the angle Θ_f.[24] The angular distribution for the partially conserved parallel momentum is most simply given by the integral

$$P(\Theta_f) = \frac{\cos\Theta_f \int_0^E dE_{\rm trans} e^{-(\sqrt{E_{\rm trans}}\sin\Theta_f - \sqrt{E_i}\sin\Theta_i)^2/\beta} \int_0^{E-E_{\rm trans}} d\epsilon\, \epsilon^{-\xi} (E - E_{\rm trans} - \epsilon)^{n-1}}{\int_{-1}^1 d\sin\Theta_f \int_0^E dE_{\rm trans} e^{-(\sqrt{E_{\rm trans}}\sin\Theta_f - \sqrt{E_i}\sin\Theta_i)^2/\beta} \int_0^{E-E_{\rm trans}} d\epsilon\, \epsilon^{-\xi} (E - E_{\rm trans} - \epsilon)^{n-1}}$$
$$= \frac{\cos\Theta_f \int_0^E dE_{\rm trans} e^{-(\sqrt{E_{\rm trans}}\sin\Theta_f - \sqrt{E_i}\sin\Theta_i)^2/\beta} (E - E_{\rm trans})^{n-\xi}}{\int_{-1}^1 dx \int_0^E dE_{\rm trans} e^{-(x\sqrt{E_{\rm trans}} - \sqrt{E_i}\sin\Theta_i)^2/\beta} (E - E_{\rm trans})^{n-\xi}} \tag{A14}$$

and the $\langle E_f\rangle$ $(=\langle E_{\rm trans}\rangle)/E_i$ distribution is given by an additional factor of $E_{\rm trans}$ inside the integral in the numerator. Once again, flux detection requires that n be changed to $n+1/2$. In our calculations of these distributions the integrals are performed numerically.[30]

[1] A. W. Kleyn, A. C. Luntz, and D. J. Auerbach, Phys. Rev. Lett. **47**, 1169 (1981); Surf. Sci. **117**, 33 (1982).
[2] A. W. Kleyn and T. C. M. Horn, Phys. Rep. **199**, 191 (1991).
[3] M. G. Tenner, F. H. Geuzebroek, E. W. Kuipers, A. E. Wiskerke, A. W. Kleyn, S. Stolte, and A. Namiki, Chem. Phys. Lett. **168**, 45 (1990); F. H. Geuzebroek, A. E. Wiskerke, M. G. Tenner, A. W. Kleyn, S. Stolte, and A. Namiki, J. Phys. Chem. **95**, 8409 (1991).
[4] K. R. Lykke and B. D. Kay, J. Phys. Condens. Matter **3**, S65 (1991); J. Chem. Phys. **92**, 2614 (1990).
[5] T. F. Hanisco, C. Yan, and A. C. Kummel, J. Chem. Phys. **97**, 1484 (1992); J. Vac. Sci. Technol. A **11**, 2090 (1993).
[6] G. O. Sitz, A. C. Kummel, and R. N. Zare, J. Chem. Phys. **87**, 3247 (1987); G. O. Sitz, A. C. Kummel, R. N. Zare, and J. C. Tully, *ibid*. **89**, 2572 (1988).
[7] M. A. Hines and R. N. Zare, J. Chem. Phys. **98**, 9134 (1993).
[8] A. C. Kummel, G. O. Sitz, R. N. Zare, and J. C. Tully, J. Chem. Phys. **89**, 6947 (1988); **91**, 5793 (1989).
[9] G. O. Sitz, A. C. Kummel, and R. N. Zare, J. Chem. Phys. **89**, 2558 (1988).
[10] D. C. Jacobs, K. W. Kolasinski, R. J. Madix, and R. N. Zare, J. Chem. Phys. **87**, 5038 (1987).
[11] D. C. Jacobs, K. W. Kolasinski, S. F. Shane, and R. N. Zare, J. Chem. Phys. **85**, 5469 (1986).
[12] A. C. Luntz, A. W. Kleyn, and D. J. Auerbach, Phys. Rev. B **25**, 4273 (1982).
[13] A. W. Kleyn, A. C. Luntz, and D. J. Auerbach, Surf. Sci. **152/153**, 99 (1985).
[14] T. F. Hanisco and A. C. Kummel, J. Chem. Phys. **99**, 7076 (1993).
[15] T. F. Hanisco and A. C. Kummel, J. Vac. Sci. Technol. **11**, 1907 (1993).
[16] A. E. Wiskerke, C. A. Taatjes, A. W. Kleyn, R. J. W. E. Lahaye, S. Stolte, D. Bronnikov, and B. E. Hayden, J. Chem. Phys. **102**, 3835 (1995).
[17] J. B. C. Pettersson, G. Nyman, and L. Holmlid, J. Chem. Phys. **89**, 6963 (1988).
[18] G. Nyman, L. Holmlid, and J. B. C. Pettersson, J. Chem. Phys. **93**, 845 (1990).
[19] J. B. C. Pettersson, J. Chem. Phys. **100**, 2359 (1994).
[20] A. E. Wiskerke, C. A. Taatjes, A. W. Kleyn, R. J. W. E. Lahaye, S. Stolte, D. Bronnikov, and B. E. Hayden, Chem. Phys. Lett. **216**, 93 (1993).
[21] A. E. Wiskerke, C. A. Taatjes, A. W. Kleyn, R. J. W. E. Lahaye, S. Stolte, D. K. Bronnikov, and B. E. Hayden, Faraday Discuss. **96**, 297 (1993).
[22] A. E. Wiskerke and A. W. Kleyn (to be published).
[23] E. Zamir and R. D. Levine, Chem. Phys. Lett. **104**, 143 (1984).
[24] H.-D. Meyer and R. D. Levine, Chem. Phys. **85**, 189 (1984).
[25] H. Kang, K. H. Park, S. H. Suck Salk, and C. W. Lee, Chem. Phys. Lett. **193**, 104 (1992).
[26] A. Ben-Shaul, R. D. Levine, and R. B. Bernstein, J. Chem. Phys. **61**, 4937 (1974).
[27] R. A. Marcus, Philos. Trans. R. Soc. London Ser. A **332**, 283 (1990); P. Pechukas and J. C. Light, J. Chem. Phys. **42**, 3281 (1965).
[28] W. Forst, *Theory of Unimolecular Reactions* (Academic, New York, 1973).
[29] R. B. Bernstein and R. D. Levine, Adv. At. Mol. Phys. **11**, 215 (1975).
[30] IMSL routine BETAI was used; see also, for example, W. H. Press, S. A. Teukolsky, and W. T. Vetterling, *Numerical Recipes in C: The Art of Scientific Computing* (Cambridge University, Cambridge, 1972).
[31] A. C. Kummel, G. O. Sitz, and R. N. Zare, J. Chem. Phys. **85**, 6880 (1986); **88**, 6707 (1988).
[32] IMSL routines QDAGS and TWODQ were used.
[33] NO–Pt(111), C. T. Campbell, G. Ertl, and J. Segner, Surf. Sci. **115**, 309 (1982); J. A. Serri, J. C. Tully, and M. J. Cardillo, J. Chem. Phys. **79**, 1531 (1983); N_2–W(110), J. T. Yates, R. Klein, and T. E. Madey, Surf. Sci. **56**, 469 (1976).
[34] H. E. Pfnür, C. T. Rettner, J. Lee, R. J. Madix, and D. J. Auerbach, J. Chem. Phys. **85**, 7452 (1986).
[35] J. K. Brown and A. C. Luntz, Chem. Phys. Lett. **204**, 451 (1993).
[36] J. Harris and A. C. Luntz, J. Chem. Phys. **91**, 6421 (1989).
[37] J. C. Polanyi and R. J. Wolf, Ber. Bunsenges. Phys. Chem. **86**, 356 (1982); J. Chem. Phys. **82**, 1555 (1985).
[38] D. C. Jacobs and R. N. Zare, J. Chem. Phys. **91**, 3196 (1989).
[39] P. J. van den Hoek and A. W. Kleyn, J. Chem. Phys. **91**, 4318 (1989).
[40] E. W. Kuipers, M. G. Tenner, A. W. Kleyn, and S. Stolte, Phys. Rev. Lett. **62**, 2152 (1989); M. G. Tenner, E. W. Kuipers, A. W. Kleyn, and S. Stolte, J. Chem. Phys. **94**, 5197 (1991).
[41] H. Voges and R. Schinke, Chem. Phys. Lett. **95**, 221 (1983); **100**, 245 (1983).
[42] I. S. Gradshteyn and I. M. Ryzhik, *Table of Integrals, Series, and Products*, 4th ed. (Academic, New York, 1965).
[43] G. Comsa and R. David, Surf. Sci. Rep. **5**, 145 (1985).